

Supplementary Information

A Chameleonic Macrocyclic Peptide with Drug Delivery Applications

Colton D. Payne^a, Bastian Franke^a, Mark F. Fisher^b, Fatemeh Hajiaghaalipour^a, Courtney E. McAleese^a, Angela Song^a, Carl Eliasson^a, Jingjing Zhang^b, Achala S. Jayasena^b, Grishma Vadlamani^b, Richard J. Clark^a, Rodney F. Minchin^a, Joshua S. Mylne^b & K. Johan Rosengren^{a,*}

^aThe University of Queensland, School of Biomedical Sciences, Brisbane, QLD 4072, Australia

^bThe University of Western Australia, School of Molecular Sciences & The ARC Centre of Excellence in Plant Energy Biology, Crawley, WA 6009, Australia

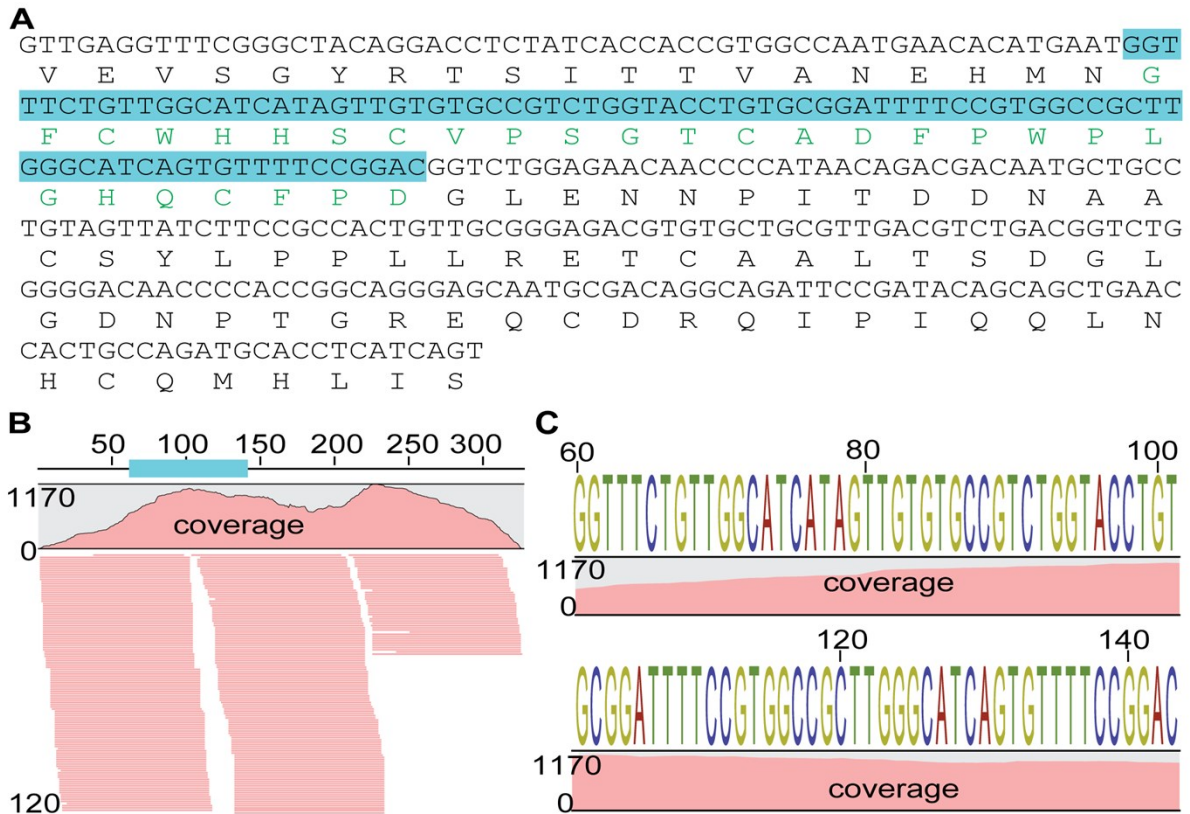


Fig S1. Contig sequence that encodes PDP-23 and sequence support. (A) Sequence assembled de novo from RNA-seq of *Zinnia elegans* seeds that encodes PDP-23 (cyan highlight) and its translated sequence. (B) Mapping RNA-seq reads to the contig shows strong support for the sequence with the average depth of coverage being 696 reads. (C) The sequence logo generated from mapped reads shows high confidence for the PDP-23 sequence with no evidence for sequence polymorphism.

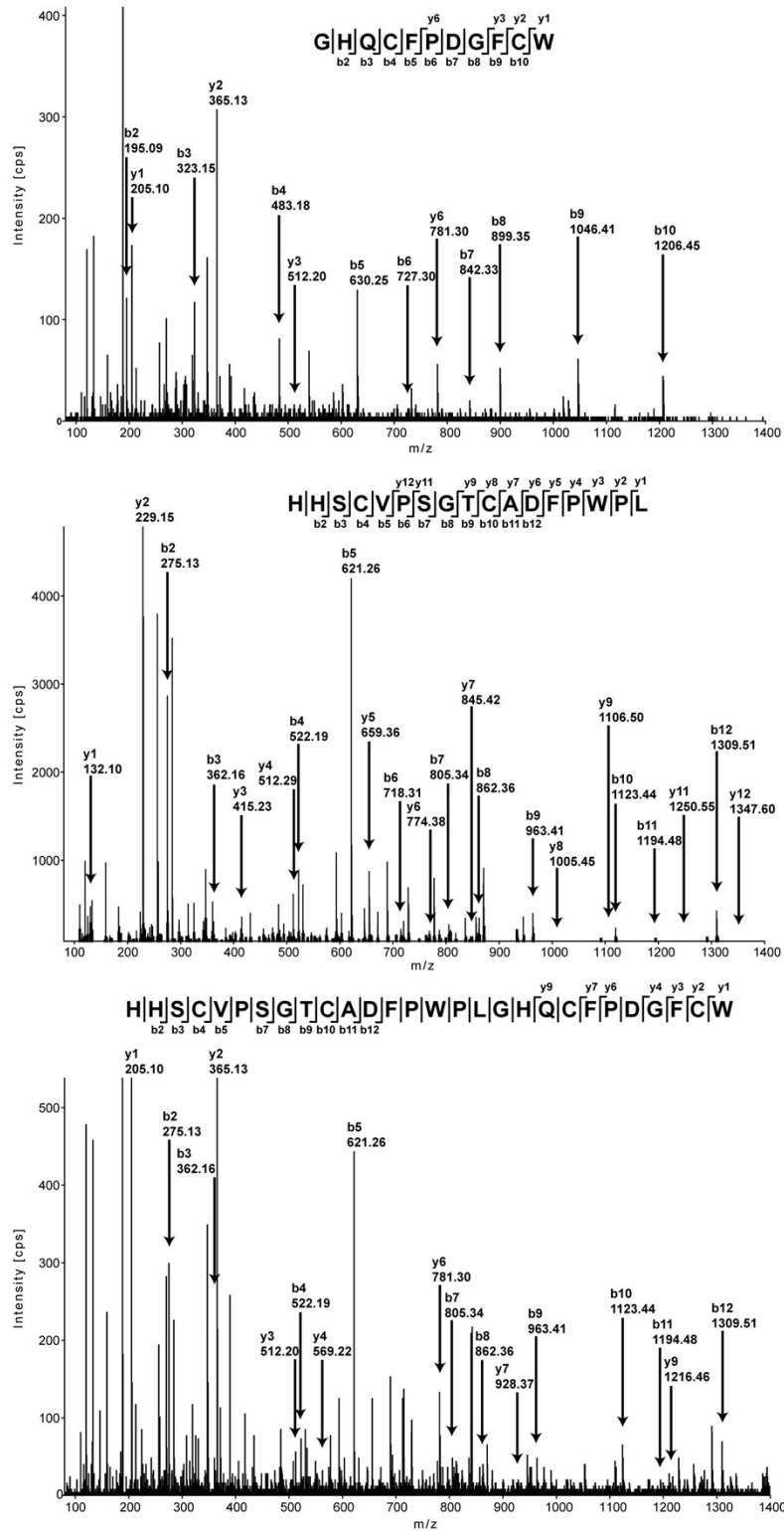


Fig S2. MS/MS sequencing of the PDP-23 enriched extract digested with chymotrypsin. The b- and y-ions are shown of the three identified fragments after the PDP-23 enriched extract was reduced, alkylated and digested with chymotrypsin.

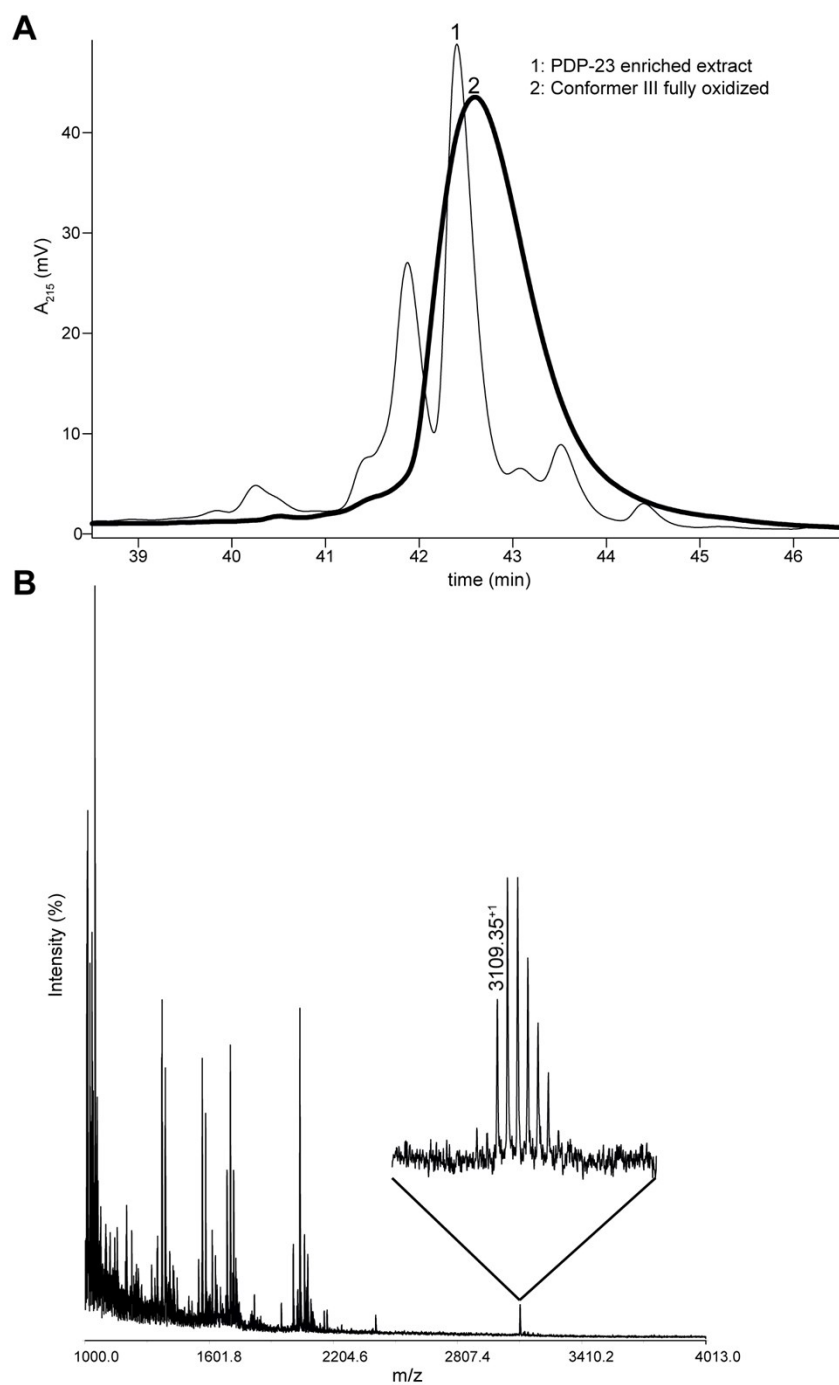


Fig S3. Analytical HPLC profile of isomer III and PDP-23 enriched extract. (A) Analytical HPLC trace of conformer III highlighted in a solid bold black line overlaid with a trace of PDP-23 enriched extract. (B) MALDI-TOF mass spectrum showing the mass-to-charge ratio (m/z) of PDP-23 alongside many other masses in the PDP-23 enriched extract.

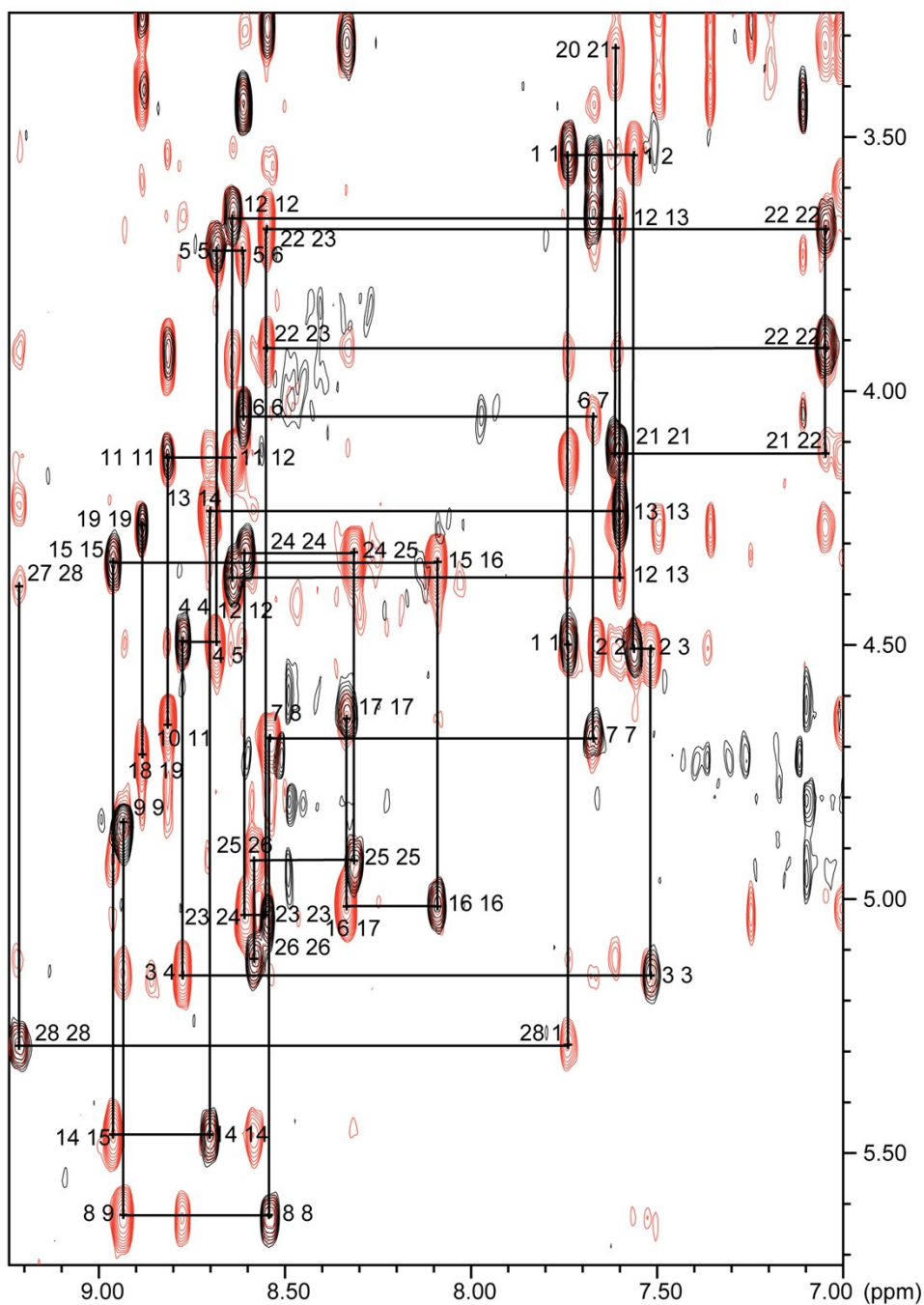


Fig S4. Sequential assignment of the NMR data. The ‘sequential walk’ in the ‘fingerprint’ H_{α} -HN region of the NMR spectra is shown for PDP-23. Data were recorded in 90:10 (H_2O/D_2O) at 600 MHz and 298 K. The TOCSY spectrum (80 ms mixing time; black), which contain only intra-residual connections is superimposed on the NOESY spectrum (200 ms mixing time; red), which contain both intra- and inter-residual connections. The sequential walk is only broken by proline residues at positions 10, 18, 20, 27.

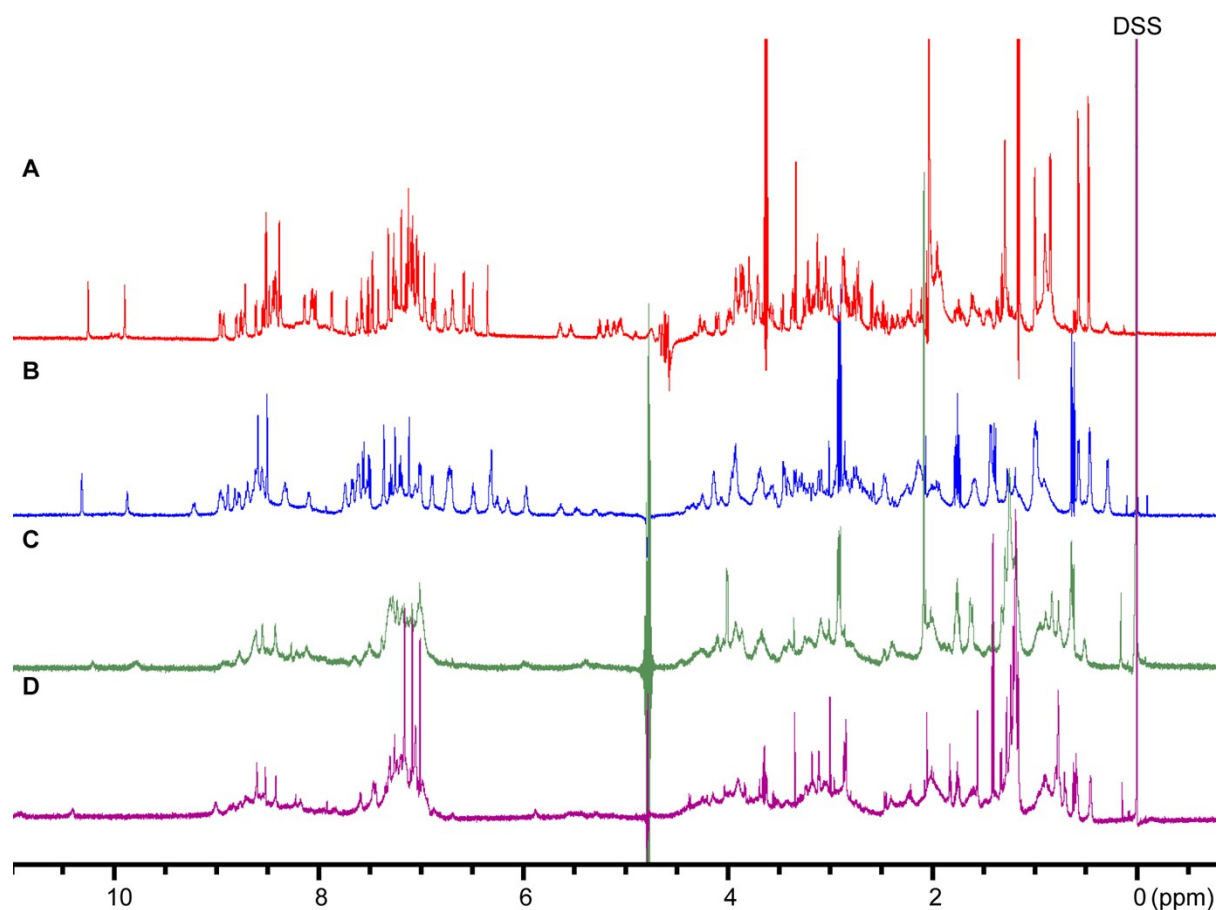


Fig S5. One-dimensional ^1H NMR spectra of PDP-23 in different environments. (A) PDP-23 in 80:20 ($\text{H}_2\text{O}/\text{CD}_3\text{CN}$), (B) PDP-23 in 90:10 ($\text{H}_2\text{O}/\text{D}_2\text{O}$), (C) PDP-23 when exposed to SDS micelles, (D) PDP-23 when exposed to DPC micelles. All spectra were recorded at 298K, and are aligned to DSS at 0 ppm.

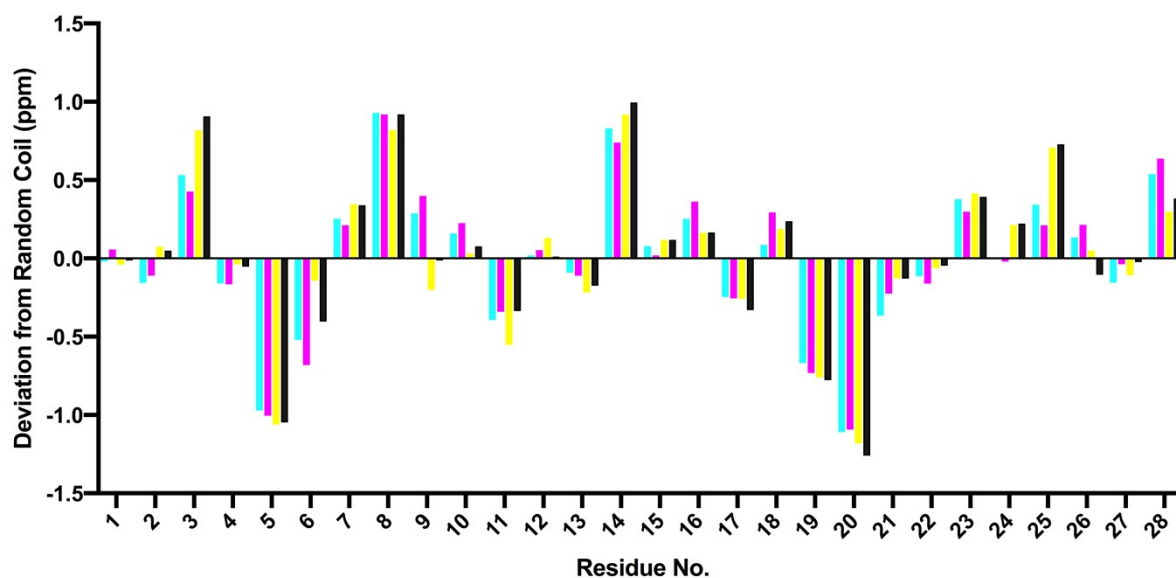


Fig S6. Secondary H_{α} chemical shifts of PDP-23 in different environments. Secondary shifts, the difference between observed chemical shifts and chemical shifts observed in short unstructured random coil peptides, are sensitive indicators of secondary structure. Negative values are typical of helical or turn structure, while positive values suggest extended sheet structure. Columns are color coded according to conditions; 80:20 H_2O/CD_3CN (cyan), 90:10 (H_2O/D_2O) (magenta), SDS micelles (yellow), DPC micelles (black). The secondary shifts are remarkably similar, confirming the secondary structure is largely the same.

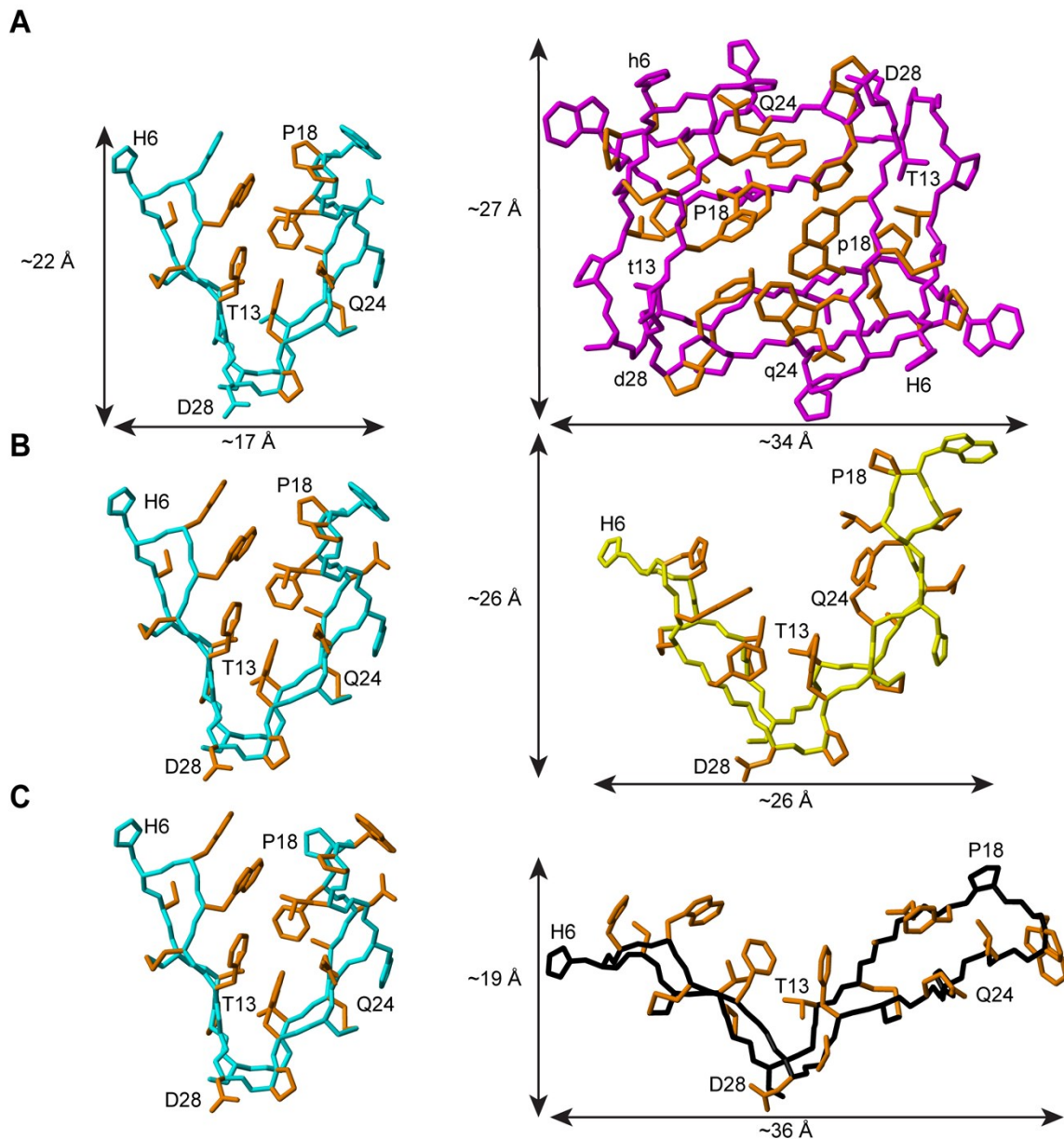


Fig S7. Three-dimensional structures of PDP-23 in different environments. (A) Comparison of key structural differences between monomeric PDP-23 when in 80:20 H₂O/CD₃CN and dimeric PDP-23 when in 90:10 H₂O/D₂O. PDP-23 in (80:20) H₂O/CD₃CN is colored cyan, PDP-23 in 90:10 H₂O/D₂O is colored magenta. Sidechains of residues showing chemical shift differences >0.15 ppm between the two conditions are highlighted in orange in both structures, reflecting changes in the core. (B) Comparison of key structural differences between PDP-23 when in (80:20) H₂O/CD₃CN and when exposed to SDS micelles. PDP-23 in 80:20 H₂O/CD₃CN is colored cyan, PDP-23 exposed to SDS micelles is colored yellow. Residues with chemical shift deviations >0.15 ppm are highlighted in orange in both structures. (C) Comparison of key structural differences between PDP-23 when in 80:20 H₂O/CD₃CN and when exposed to DPC micelles. PDP-23 in 80:20 H₂O/CD₃CN is colored cyan, PDP-23 exposed to DPC micelles is colored black. Residues with chemical shift deviations >0.15 ppm are highlighted in orange in both structures. For all structures residue labels are supplied for orientation in the case of PDP-23 in 90:10 H₂O/D₂O capital and non-capital letters are used to denote individual monomers.

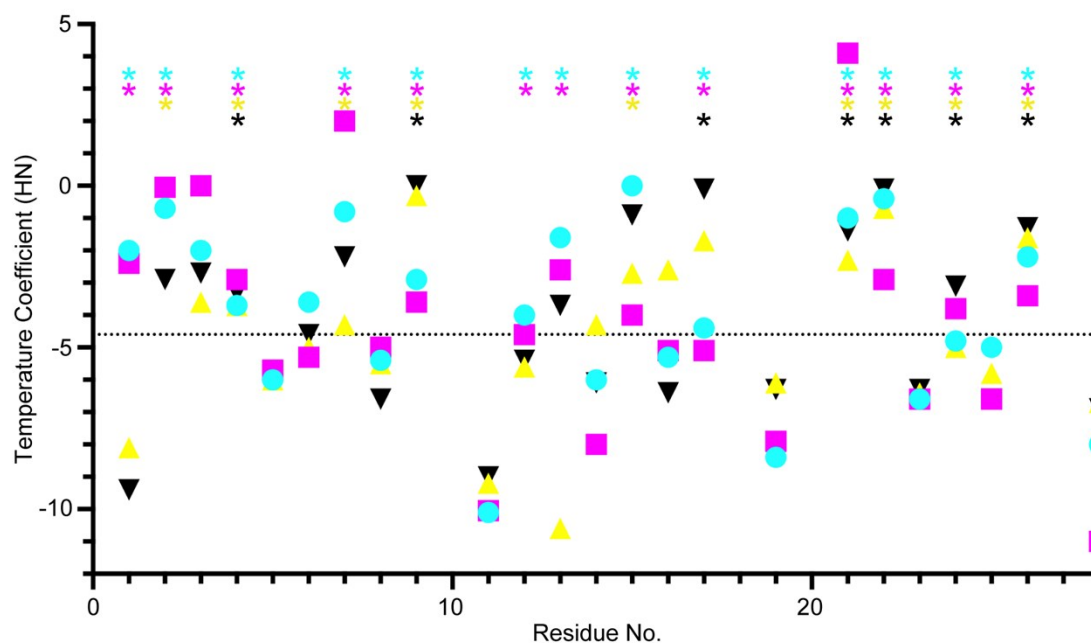


Fig S8. Amide proton temperature coefficients for PDP-23 in different environments. Amide protons involved in hydrogen bonds are protected from solvent and their chemical shift is less affected by temperature changes. For amide protons with a temperature coefficient >-4.6 ppb/K (indicated by the dashed line) the likelihood of being involved in a hydrogen bond is $>86\%$ ¹. Data points are color coded according to conditions; 80:20 H₂O/CD₃CN (cyan), 90:10 (H₂O/D₂O) (magenta), SDS micelles (yellow), DPC micelles (black). Hydrogen bonds with confirmed unambiguous acceptors are highlighted by * at the top, and in all cases, these are consistent between conditions. Based on temperature coefficient analysis the majority of hydrogen bonds are unaffected by condition changes, but residues like Gly1 and Thr13 do show a larger change in temperature dependence indicating hydrogen bonds are being broken in micelles.

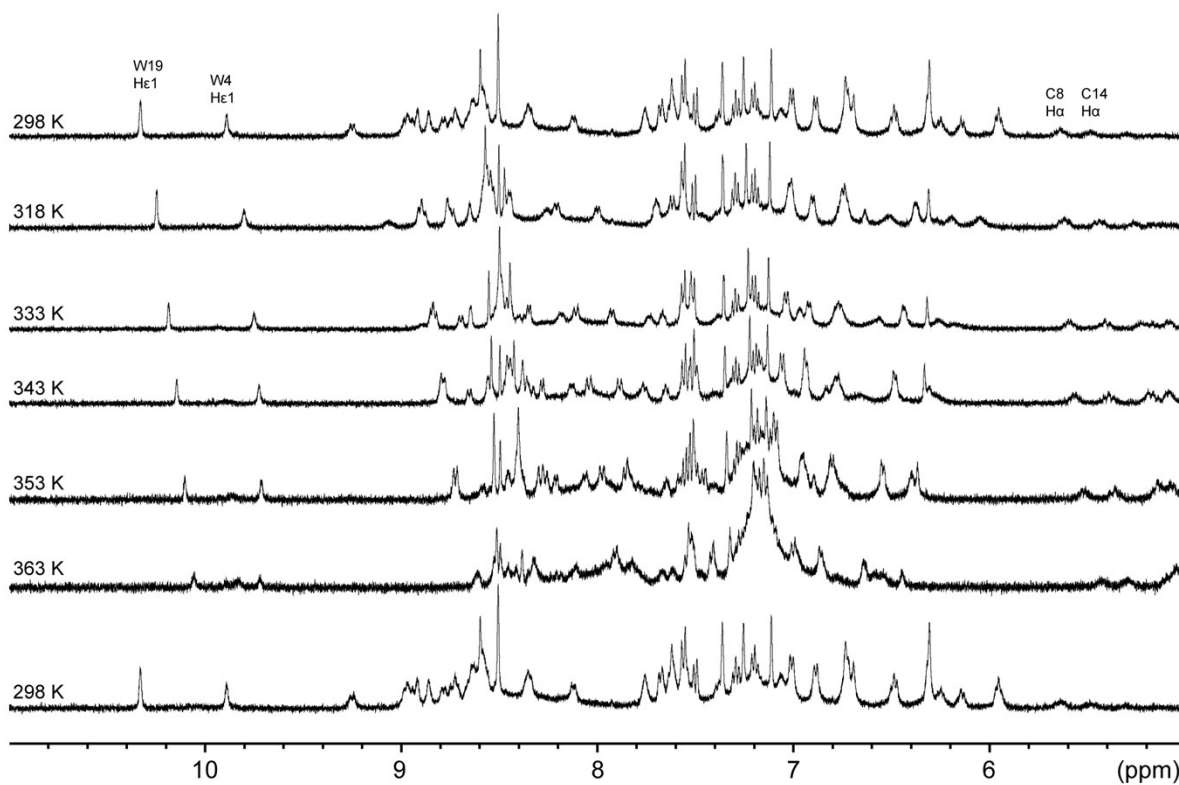


Fig S9. One-dimensional ¹H NMR spectra showing thermal stability of PDP-23. 1D ¹H NMR spectra of PDP-23 recorded while cycling the temperature from 298-363-298 K. Data show only partial denaturing effects at a temperature of 363 K at the two tryptophan indole signals and Cys H α signals. In contrast, aromatic signals around 5.8-6.5 ppm, which are generated from the packing of Phe sidechains in the dimer core, move downfield, consistent with the effect of addition of acetonitrile and separation into monomers. The complete reversibility of thermal denaturation was confirmed when the temperature was again decreased to 298 K, with the 1D spectrum being identical to the 1D spectrum prior to heating.

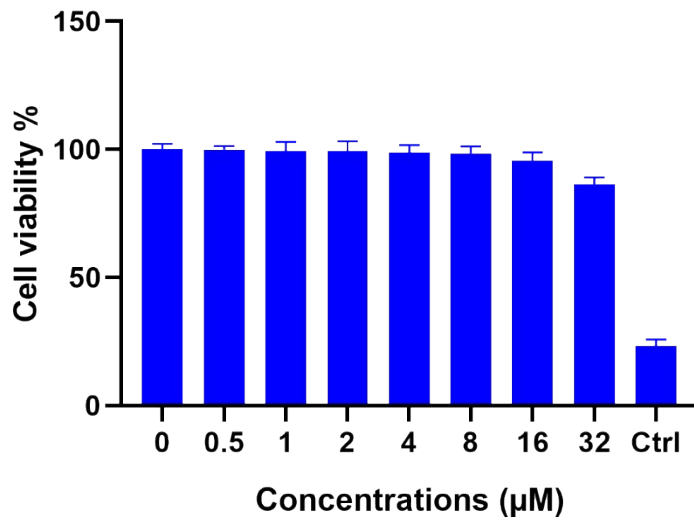


Fig S10. Cell viability of HeLa cells exposed to PDP-23 for 48 hours. Cells were incubated in a serial dilution of PDP-23 for 48 h and cell viability was then determined by MTT assay. Cells treated with 5% (v/v) DMSO were used as a positive control. The assay was performed in triplicate and the results are presented as the means \pm SD.

Table S1. Structural Statistics of PDP-23 in different environments

	80:20 H ₂ O/CD ₃ CN	90:10 H ₂ O/D ₂ O	SDS micelles	DPC micelles
Energies (kcal/mol)				
Overall	-801.1 ± 12.0	-1743.1 ± 36.0	-789.7 ± 21.4	-770.7 ± 37.5
Bonds	12.60 ± 0.98	20.97 ± 1.17	11.74 ± 1.27	11.22 ± 1.02
Angles	38.26 ± 2.07	54.07 ± 4.78	31.37 ± 4.13	32.45 ± 8.90
Improper	13.36 ± 1.59	21.86 ± 2.85	14.56 ± 3.87	12.99 ± 4.09
Dihedral	121.8 ± 1.38	238.8 ± 1.63	119.1 ± 1.26	119.8 ± 2.26
Van der Waals	-96.51 ± 3.02	-272.3 ± 8.71	-97.43 ± 7.75	-98.59 ± 10.9
Electrostatic	-891.1 ± 10.8	-1806.8 ± 30.3	-869.5 ± 19.5	-848.9 ± 32.8
NOE	0.16 ± 0.02	0.07 ± 0.06	0.36 ± 0.97	0.06 ± 0.05
Cdih	0.42 ± 0.21	0.22 ± 0.15	0.18 ± 0.57	0.17 ± 0.12
MolProbity Statistics				
Clashes (>0.4 Å/1000 atoms)	15.7 ± 4.6	11.5 ± 2.5	12.8 ± 3.8	12.6 ± 4.4
Poor Rotamers	0	0.3 ± 0.5	0	0.5 ± 0.6
Ramachandran Outliers (%)	0	0	1.2 ± 1.8	2.9 ± 3.3
Ramachandran Favored (%)	97.7 ± 1.9	97.7 ± 1.8	93.7 ± 5.2	81.2 ± 5.6
MolProbity Score	1.84 ± 0.2	1.64 ± 0.1	1.94 ± 0.3	2.52 ± 0.4
MolProbity score percentile	82.7 ± 8.5	91.0 ± 3.8	77.0 ± 13.3	47.4 ± 18.6
Atomic RMSD (Å)				
Mean Global Backbone	0.43 ± 0.11	0.73 ± 0.15	1.60 ± 0.50	1.82 ± 0.63
Mean Global Heavy	0.92 ± 0.15	1.28 ± 0.15	2.66 ± 0.61	2.78 ± 0.82
Experimental Restraints				
Distance Restraints				
Short range (i-j < 2)	217	436	211	192
Medium range (i-j < 5)	74	114	39	44
Long range (i-j > 5)	115	192	77	59
Intermolecular		162		
Hydrogen bonds	26	52	20	12
	(13 H-bonds)	(26 H-bonds)	(10 H-bonds)	(6 H-bonds)
Total	432	956		307
Dihedral Restraints				
Φ	18	40	3	11
Ψ	20	44	2	11
Total	38	84	5	22
Restraint violations				
Total NOE violations > 0.2 Å	0	0	0	0
Total Dihedral violations > 2.0°	0	0	0	0

Table S2. Chemical Shift Differences between 90:10 (H₂O/D₂O) and 80:20 (H₂O/CD₃CN)

Residue	Atom	$\Delta\delta$ (H ₂ O/D ₂ O)-(H ₂ O/CD ₃ CN) (≥ 0.15 ppm are listed)
1	HA3	-0.178
2	HB2	0.284
2	QD	0.248
2	HN	0.166
3	HB3	0.206
4	HD1	0.412
4	HB2	0.259
4	HB3	0.259
4	HZ3	-0.29
4	HZ2	-0.373
4	HH2	-0.448
4	CB	1.559
6	HA	0.16
6	HN	-0.226
7	HB3	0.265
7	HB2	0.254
7	HN	0.2
9	HB	-0.273
11	HN	-0.287
12	HN	-0.176
14	HB3	0.333
14	HN	-0.265
14	CB	1.131
15	QB	0.595
16	CB	2.376
16	CA	1.446
17	HZ	0.709
17	QE	0.614
17	QD	0.257
17	HB2	-0.193
17	HN	-0.244
17	CB	1.383
18	HG2	-0.156
18	HD2	-0.162
18	HA	-0.207
20	HB3	-0.228
21	HN	0.525
21	HB2	0.293
21	HG	0.173
21	HB3	0.153
22	HN	-0.294
24	HE21	0.289
24	HE22	0.193
24	HG3	-0.355
25	HN	0.263
26	QD	-0.151
26	HZ	-0.373
26	QE	-0.714
27	HD3	0.325
27	HD2	0.308
27	HB3	0.16
27	CA	1.947
27	CB	1.527
28	HN	0.414
28	CB	1.823
28	CA	1.092

Table S3. Chemical shift differences between 90:10 (H₂O/D₂O) and SDS/DPC micelles. * denotes the difference being <0.15 ppm

Residue	Atom	$\Delta\delta$ (H ₂ O/D ₂ O)-(H ₂ O/SDS), (H ₂ O/D ₂ O)-(H ₂ O/DPC) (>0.15 ppm are listed)
1	HA3	0.31, 0.37
1	HA2	*, -0.22
1	HN	-0.38, -0.58
2	HA	-0.19, *
2	HN	*, -0.27
2	HE*	-0.279, -0.453
2	HD*	-0.638, -0.735
2	HB2	-0.82, -0.8
2	HB3	-1.25, -1.134
2	CB	1.154, 3.949
3	HA	-0.219, -0.302
3	HB3	-0.298, -0.215
3	HB2	-0.332, 0.295
3	HN	-0.562, -0.656
4	HH2	0.536, 0.583
4	HZ3	0.351, 0.394
4	HZ2	0.301, 0.273
4	HE3	0.171, 0.199
4	HB3	-0.366, -0.291
4	HB2	-0.419, -0.384
4	HD2	-0.575, -0.547
4	HE1	*, -0.539
4	HN	*, -0.242
4	CB	1.709, 4.504
5	HD2	0.338, 0.421
5	HB3	0.216, *
5	HB2	0.173, *
5	HN	*, -0.311
5	CA	*, 3.006
5	CB	*, 1.986
6	HN	0.195, *
6	HA	-0.538, -0.263
6	CA	*, 1.765
6	CB	-1.03, *
7	HB3	-0.336, -0.331
7	HB2	-0.36, -0.412
7	HN	-0.52, -0.498
7	CA	*, 2.522
8	HA	0.258, 0.163
8	HN	*, -0.162
8	CA	*, -5.809
8	CB	-8.604, *
9	HB	0.957, 0.774
9	HA	0.593, 0.577
9	HG2*	0.308, 0.284
9	HG1*	0.254, 0.238
9	HN	0.179, 0.162
10	HA	0.214, 0.162
10	HG3	0.202, 0.178
11	CA	*, 2.89
12	HA2	0.272, *
13	HG*	0.168, 0.191
13	HN	-0.291, -0.966
13	CB	*, 2.6
14	HN	0.2, *
14	HB3	-0.44, -0.418
15	HB*	-0.555, -0.498
15	CA	*, 2.613
15	CB	7.354, *
16	HA	0.205, 0.208
16	HB3	-0.29, -0.28
16	HB2	-0.291, -0.28

16	HN	*, -0.677
16	CB	2.912, 5.707
17	HN	0.718, 0.728
17	HB2	*, -0.191
17	HD*	-0.301, -0.299
17	HE*	-0.689, 0.663
17	HZ	-0.879, -0.824
17	CA	*, 5.004
17	CB	2.209, *
18	HG3	0.182, *
19	HZ3	*, 0.244
19	HH2	*, 0.167
19	HE1	*, -0.598
19	CA	-1.913, *
20	HD2	1.851, 0.25
20	HD3	1.69, *
20	HG2	0.416, 0.188
20	HG3	*, 0.514
20	HB3	0.309, 0.646
20	HA	*, 0.187
20	CA	*, -9.006
21	HG	*, 0.156
21	HB3	-0.288, -0.264
21	HB2	-0.324, -0.326
21	HN	-0.532, -0.618
21	CA	-2.427, *
22	HN	*, 0.178
22	HA3	-0.177, -0.167
23	HN	0.16, *
23	CB	*, 2.731
24	HE21	0.222, 0.236
24	HE22	0.181, *
24	HA	-0.239, -0.228
24	HB3	-0.252, -0.408
24	HB2	-0.419, -0.238
24	HG3	-0.482, -0.411
24	HG2	-0.452, -0.461
24	CA	-2.222, *
25	HA	-0.342, -0.338
25	CA	*, 1.865
26	HA	0.159, 0.324
26	HB3	-0.178, -0.174
26	HB2	-0.232, *
26	HD*	-0.368, -0.306
26	HZ	-0.919, -0.835
26	HE*	-1.14, -1.09
27	HD2	0.325, 0.495
27	HD3	0.257, 0.281
27	CA	*, 3.628
28	HN	0.597, 0.496
28	HA	0.34, 0.275
28	HB3	-0.31, *
28	CB	-8.252, -5.457

Supplementary Reference

1. Cierpicki, T. & Otlewski, J. Proton temperature coefficients as hydrogen bond indicators in proteins. *J. Biomol. NMR.* 21, 249-261, (2001).